MOL PHARM

Dual Role of the Second Extracellular Loop of the Cannabinoid Receptor 1: Ligand Binding and Receptor Localization

Kwang H. Ahn, Alexander C. Bertalovitz, Dale F. Mierke, and Debra A. Kendall

Department of Molecular and Cell Biology, University of Connecticut, Storrs, Connecticut (K.H.A., A.C.B, D.A.K.); Department of Chemistry, Dartmouth College, Hanover, New Hampshire (D.F.M)

MOLECULAR PHARMACOLOGY

ABSTRACT

The seven transmembrane α-helices of G protein-coupled receptors (GPCRs) are the hallmark of this superfamily. Intrahelical interactions are critical to receptor assembly and, for the GPCR subclass that binds small molecules, ligand binding. Most research has focused on identifying the ligand binding pocket within the helical bundle, whereas the role of the extracellular loops remains undefined. Molecular modeling of the cannabinoid receptor 1 (CB1) extracellular loop 2 (EC2), however, suggests that EC2 is poised for key interactions. To test this possibility, we employed alanine scanning mutagenesis of CB1 EC2 and identified two distinct regions critical for ligand binding, G protein coupling activity, and receptor trafficking. Receptors with mutations in the N terminus of EC2 (W255A, N256A) were retained in the endoplasmic reticulum and did not bind the agonist (1*R*,3*R*,4*R*)-3-[2-hydroxy-4-(1,1-dimethylheptyl)-phenyl]-4-(3-hydroxypropyl)cyclohexan-1-ol (CP55940) or the inverse agonist *N*-(piperidin-1-yl)-5-(4-chlorophenyl)-1-(2,4-dichlorophenyl)-4-methyl-1*H*-pyrazole-3-carboxamide (SR141716A). In contrast, the C terminus of EC2 differentiates agonist and inverse agonist; the P269A, H270A, and I271A receptors exhibited diminished binding for several agonists but bound inverse agonists SR141716A, *N*-(piperidin-1-yl)-5-(4-iodophenyl)-1-(2,4-dichlorophenyl)-4-methyl-1*H*-pyrazole-3-carboxamide (AM251), and 4-[6-methoxy-2-(4-methoxyphenyl)-benzofuran-3-carbonyl]benzonitrile (LY320135) with wild-type receptor affinity. The F268A receptor involving substitution in the Cys-X-X-X-Ar motif, displayed both impaired localization and ligand binding. Other amino acid substitutions at position 268 revealed that highly hydrophobic residues are required to accomplish both functions. It is noteworthy that a F268W receptor was trafficked to the cell surface yet displayed differential binding preference for inverse agonists comparable with the P269A, H270A, and I271A receptors. The findings are consistent with a dual role for EC2 in stabilizing receptor assembly and in ligand binding.

The human cannabinoid receptor 1 (CB1) is a member of the rhodopsin-like G protein-coupled receptor (GPCR) family, members of which comprise seven transmembrane helices (TMs) connected by three intracellular loops and three extracellular loops. In addition to binding Δ⁹-tetrahydrocannabinol (Δ⁹-THC), the psychoactive constituent of *Cannabis sativa*, several endogenous cannabinoid receptor agonists have been identified, including anandamide (arachidonoylethanolamide), 2-arachidonoylglycerol, and 2-arachidonylglyceryl ether (noladin ether). CB1 also binds a variety of synthetic cannabimimetic compounds such as the nonclassic agonist CP55940, a bicyclic analog of Δ⁹-THC, the classic agonist HU-210, and the selective inverse agonists SR141716A (also known as rimonabant), AM251, and LY320135. Upon activation, CB1 modulates synaptic transmission, ultimately playing a role in analgesia, anxiety, feeding behavior, and movement disorders (Porter and Felder, 2001; Howlett et al., 2002). Thus, understanding the features of CB1 critical for ligand binding and receptor localization is important for developing its therapeutic potential.

Molecular modeling analyses of ligand-receptor interactions involving CB1 are consistent with the idea that the

ABBREVIATIONS: CB1, cannabinoid receptor 1; GPCR, G protein-coupled receptor; TM, transmembrane helices; EC2, extracellular loop 2; CP55940, (1*R*,3*R*,4*R*)-3-[2-hydroxy-4-(1,1-dimethylheptyl)-phenyl]-4-(3-hydroxypropyl)cyclohexan-1-ol; methanandamide, (*R*)-*N*-(2-hydroxy-1-methylethyl)-5*Z*,8*Z*,11*Z*,14*Z*-eicosatetraenamide; SR141716A, *N*-(piperidin-1-yl)-5-(4-chlorophenyl)-1-(2,4-dichlorophenyl)-4-methyl-1*H*-pyrazole-3-carboxamide; HU-210, (−)-(6a*R*)-*trans*-3-(1,1-dimethylheptyl)-6a,7,10,10a-tetrahydro-1-hydroxy-6,6-dimethyl-6*H*-dibenzo[*b,d*]pyran-9-methanol; AM251, *N*-(piperidin-1-yl)-5-(4-iodophenyl)-1-(2,4-dichlorophenyl)-4-methyl-1*H*-pyrazole-3-carboxamide; LY320135, 4-[6-methoxy-2-(4-methoxyphenyl)benzofuran-3-carbonyl]benzonitrile; HEK293T, human embryonic kidney cell; PBS, phosphate-buffered saline; TME, Tris/Mg²⁺/EDTA; GTPγS, guanosine 5′-3-*O*-(thio)triphosphate; ER, endoplasmic reticulum; GFP, green fluorescent protein; PDI, protein disulfide isomerase.

binding pocket is primarily hydrophobic and within the transmembrane helix bundle of the receptor, like that of other GPCRs that bind small molecules (McAllister et al., 2003). In contrast, GPCRs that bind larger ligands, such as peptide hormones, are thought to do so at the extracellular face of the receptor and typically involve interaction domains formed by the extracellular N terminus (Holtmann et al., 1995; López de Maturana et al., 2003). However, there is growing evidence that the extracellular loops are also critical for small-molecular-weight ligand recognition, selectivity, and/or entrance to the binding pocket (Shi and Javitch, 2004).

Since the crystal structure of bovine rhodopsin was solved (Palczewski et al., 2000), many homology models for the rhodopsin-like family A GPCRs, including the cannabinoid receptors, have been proposed (Shim et al., 2003; Salo et al., 2004; Montero et al., 2005). However, the structure and role of the extracellular domains are not clearly defined because of their mobility, resulting in poorly resolved diffraction patterns, and their low sequence homology, relative to the transmembrane domains. Crystal structures for the β1- and the β2-adrenergic receptors have been solved, providing insight into the structure of other GPCRs within the family (Cherezov et al., 2007; Rasmussen et al., 2007; Rosenbaum et al., 2007; Warne et al., 2008). Although the CB1 receptor belongs to the rhodopsin-like GPCR family, it shares more structural features with the β-adrenergic receptors than with rhodopsin itself. For instance, both CB1 and the β-adrenergic receptors have small noncovalently bound ligands, and both receptors share an intraloop disulfide bond formed within EC2. CB1 shares the Cys-X-X-X-Ar motif [where Ar is an aromatic residue (i.e., Phe268 in CB1)] that is conserved in EC2 among GPCRs that bind biogenic amines and peptides. This includes the V1a vasopressin receptor, where the corresponding aromatic residue, Phe209, is thought to project into the binding crevice and mutation at this position results in impaired agonist binding and intracellular signaling (Conner et al., 2007). Yet CB1 (and its receptor subtype CB2) is highly unusual in that it has only one extracellular disulfide bond residing entirely within EC2. Although this EC2 intraloop also occurs in the β-adrenergic receptors, these receptors in addition retain the disulfide between TM3 and EC2. This latter disulfide bridge is the most common among the rhodopsin-like family A receptors; most receptors of this subclass, including rhodopsin, exhibit only this bridge within the extracellular face (Karnik et al., 1988; Strader et al., 1994).

In this study, we have generated a molecular model of CB1, including EC2, that suggests residues of this extracellular loop project into the core of the receptor appropriate for key interactions with ligand and other regions of the receptor. To test this hypothesis, we used alanine-scanning mutagenesis to identify the residues of EC2 within CB1 that are critical for ligand binding. Receptors with residues sensitive to mutation were further analyzed for binding to a variety of ligands and for receptor localization. The data indicate that EC2 is a critical feature of CB1 that plays a role in its ER assembly for subsequent trafficking and in binding some classes of compounds.

Materials and Methods

CB1 Receptor Model. The model of the human CB1 receptor was built using the recently published X-ray structure of the human β2-adrenergic receptor, available as Protein Data Bank ID 2rh1 (Rasmussen et al., 2007). The backbone atoms of the transmembrane helices of human CB1 (TM1, Asn112–His143; TM2, Ser152–His181; TM3, Arg186–His219; TM4, Arg230–Trp255; TM5, Asp272–His304; TM6, Met337–Phe368; TM7, Lys376–Lys399) were template-forced to the TM helices of the β2-adrenergic receptor as defined by the X-ray structure while maintaining proper threading of the intervening loops. The α-helix in EC2 of β2-adrenergic receptor was introduced into CB1(Ser262–Ile267) based on sequence alignment. Maintaining the topological orientation observed for β2-adrenergic receptor in the X-ray structure, resulted in the side chain of Cys264 projecting toward the extracellular end of TM4 and Cys257, consistent with the disulfide bond previously ascribed to CB1 (Shire et al., 1996; Fay et al., 2005). The receptor was extensively energy-minimized first using the CVFF force field within Discover (Molecular Simulations, Inc., San Diego, CA) and then CHARMM++ within NAMD (Phillips et al., 2005). The agonist CP55940 was docked into the CB1 model guided by previous mutational and modeling studies, clearly indicating a role for Lys192 (Shim et al., 2003; Salo et al., 2004). Twenty orientations of CP55940, with the C3-alkyl tail projecting into the receptor core, as well as extracellularly, were generated and examined by molecular dynamics simulations (100 ps) followed by energy minimization.

Plasmid Construction. All mutants were generated by site-directed mutagenesis (QuikChange; Stratagene, La Jolla, CA) using the human CB1 cDNA cloned into pcDNA3.1 as a template, according to the manufacturer's instructions. All mutations were confirmed by DNA sequencing.

CB1 Expression and Membrane Preparation. HEK293T cells were cultured in Dulbecco's modified Eagle's medium supplemented with 10% fetal bovine serum and 3.5 mg/ml glucose at 37°C in 5% CO_2. For transient transfection, HEK293T cells were seeded at 8×10^5 cells/100-mm dish on the day before transfection. Transfection was carried out using the calcium phosphate precipitation method (Chen and Okayama, 1987). Membranes of transfected cells expressing the wild-type or mutant receptors were prepared as described previously (Abadji et al., 1999). In brief, 24 h after transfection, cells were harvested, washed twice with phosphate-buffered saline (PBS), and resuspended in PBS containing 4-(2-aminoethyl)benzenesulfonyl fluoride, pepstatin A, E-64, bestatin, leupeptin, and aprotinin as protease inhibitors (Sigma, St. Louis, MO). A membrane fraction was prepared by nitrogen cavitation at 750 psi for 5 min using a Parr cell disruption bomb, followed by two-step centrifugation, in which the lysate was spun at 500g at 4°C for 10 min and then the supernatant was spun at 100,000g for 40 min at 4°C. The resulting pellet was resuspended in TME buffer (25 mM Tris-HCl, 5 mM $MgCl_2$, and 1 mM EDTA, pH 7.4) containing 7% sucrose (w/v) at 0.6 μg/μl and stored at −70°C.

Radioligand Binding. Binding assays were performed as described previously (Murphy and Kendall, 2003). Approximately 30 to 40 μg of membranes were incubated at 30°C for 90 min in 200 μl of TME buffer containing 0.1% fatty acid-free bovine serum albumin using [^{3}H]CP55940 (139.6 Ci/mmol; PerkinElmer Life and Analytical Sciences, Waltham, MA) or [^{3}H]SR141716A (42 Ci/mmol; GE Healthcare, Piscataway, NJ) for both saturation and competition assays. In saturation binding assays, at least nine radiolabeled-ligand concentrations (ranging from 0.24 to 37.60 nM) were used to determine K_d values of the receptors. In competition binding assays, the cell membranes were incubated with fixed tracer concentration typically at the K_d for the receptor using at least nine concentrations of unlabeled ligands (ranging between 100 pM and 100 μM) as displacing ligands. Nonspecific binding was determined in the presence of 1 μM unlabeled ligand in most experiments. Reactions were terminated by adding 250 μl of TME containing 5% bovine serum albumin followed by filtration with a Brandel cell harvester through Whatman GF/C filter paper.

GTPγS Binding Assay. For GTPγS binding assay, 15 μg of membranes were incubated for 60 min at 30°C in GTPγS binding

assay buffer (50 mM Tris-HCl, pH 7.4, 3 mM MgCl$_2$, 0.2 mM EGTA, and 100 mM NaCl) with at least nine concentrations of unlabeled ligands (ranging between 100 pM and 100 μM), 0.1 nM [^{35}S]GTPγS (1250 Ci/mmol; PerkinElmer Life Sciences, Waltham, MA), 10 μM GDP, and 0.1% (w/v) bovine serum albumin. Nonspecific binding was determined with 10 μM unlabeled GTPγS (Sigma, St. Louis, MO). The reaction was terminated by rapid filtration through Whatman GF/C filters. A 4-ml volume of scintillation fluid was added into the vials containing dried filters and the radioactivity trapped in filters was determined by liquid scintillation counting.

Confocal Microscopy. A day after transfection, HEK293T cells expressing CB1 receptors C-terminally fused with the green fluorescent protein (GFP) were seeded onto 35-mm glass-bottomed dishes (MatTek, Ashland, MA) precoated with poly-D-lysine. Cells were washed three times with PBS and fixed with 4% paraformaldehyde for 15 min at room temperature. For colocalization studies, the cells were permeabilized by 0.1% Triton X-100 in DME containing 5% normal goat serum. After incubating with blocking solution (5% normal goat serum in DME) for 30 min at room temperature, the cells were incubated with monoclonal mouse anti-protein disulfide isomerase (anti-PDI; Affinity BioReagents, Golden, CO) diluted 1:120 in DME containing 5% normal goat serum. After washing with PBS, cells were incubated with Cy3-labeled donkey anti-mouse secondary antibody (Jackson ImmunoResearch Laboratories, West Grove, PA) diluted 1:200 for 1 h at room temperature. Cells were mounted in Vectashield mounting medium (Vector Laboratories, Burlingame, CA) and visualized using a Leica TCS SP2 confocal microscope (Leica Microsystems, Wetzlar, Germany). Images were collected from at least three independently transfected cell dishes and processed for presentation in figures using Adobe Photoshop 6.0 (Adobe Systems, San Jose, CA).

Data Analysis. All ligand binding assays and GTPγS binding assays were carried out in duplicate. Data are presented as the mean $\pm$ S.E.M value or the median with the corresponding 95% confidence limits from at least three independent experiments. The K_d and B_{max} values were calculated by nonlinear regression (fitted to a one-site binding model) and IC$_{50}$ values were determined by nonlinear regression (fitted to a one-site competition model) using Prism software (GraphPad Software Inc., San Diego, CA). K_i values were then calculated using the Cheng-Prusoff equation (Cheng and Prusoff, 1973) based on K_d values obtained from saturation binding analyses. EC$_{50}$ values for the GTPγS binding assays were calculated using a sigmoidal dose-response relationship. K_i and EC$_{50}$ values for the wild-type and mutant receptors were compared using analysis of variance followed by Dunn's post hoc test for significance. P values of < 0.05 were considered to be statistically significant.

Results

Sequence Comparisons and Molecular Modeling of EC2. The second extracellular loop of the human CB1 receptor consists of approximately 18 amino acid residues connecting TM4 and TM5 (Fig. 1A). Alignment of this sequence with the EC2 of other GPCRs (including other cannabinoid receptors) from the rhodopsin-like family (Fig. 1B) reveals several interesting features: a tryptophan occupies the N-terminal most position of EC2, consistent with its high occurrence at membrane interfaces; an intraloop disulfide bond that further constrains an already short loop is present, whereas the EC2-TM3 disulfide present in more than 90% of GPCRs in the family is absent in CB1; and the Cys-X-X-X-Ar motif is contributed by Cys264–Ser265–Asp266–Ile267–Phe268.

Molecular modeling of human CB1 was undertaken to gain insight into the possible orientation and interactions of the residues of EC2. The development of the molecular model of CB1 followed standard procedures, with the exception of

using the recent X-ray structure of the β2-adrenergic receptor in contrast to rhodopsin as employed in previous efforts (Shim et al., 2003; Salo et al., 2004). In contrast with rhodopsin, one of the fundamental differences is the presence of an α-helix in EC2 of the β2-adrenergic receptor and modeling also revealed this for CB1 (see Fig. 1, C and D). Within CB1, the central residue of this helix is Cys264, which forms a disulfide bond with Cys257 at the beginning of EC2, toward the extracellular end of TM4. The comparable helix was previously identified and characterized for the EC2 of the NK1 receptor (the substance P receptor), also a class A GPCR, from an NMR-based study examining the loop in the presence of dodecylphosphocholine (Pellegrini et al., 2001). The disulfide bond limits the conformational flexibility of EC2 keeping the residues of the C-terminal portion of EC2, in close contact with the extracellular end of the TM bundle (see Fig. 1C). The model suggests some residues are located cen-
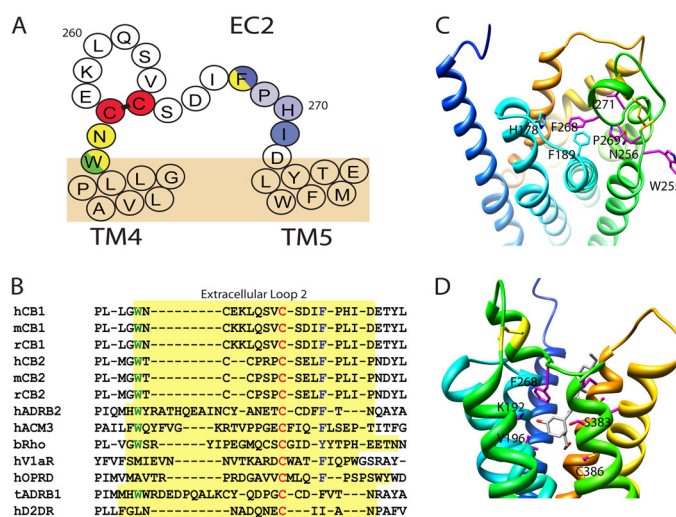

Fig. 1. Schematic diagram, sequence comparison, and molecular models of the EC2 loop region of CB1. A, schematic diagram of the EC2 loop of the human CB1 receptor. The tryptophan residue highlighted in green is highly conserved among rhodopsin-like G protein-coupled receptors. The residues that are critical for receptor trafficking are highlighted in yellow. The cluster of residues critical for CP55940 binding identified here are shown in blue. The residues most sensitive to binding multiple agonists are shaded in darker blue. The residues involved in the disulfide bond of the EC2 loop are shown in red with a black-bar linker. The lipid bilayer is represented by the beige rectangle. The residue number indicated corresponds to the position of the residue in the linear sequence. B, amino acid sequence alignment of the EC2 region (yellow) and flanking residues (unshaded) from a variety of cannabinoid and other rhodopsin-like G protein-coupled receptors: hCB1, human CB1 receptor; mCB1, mouse CB1 receptor; rCB1, rat CB1 receptor; hCB2, human CB2 receptor; mCB2, mouse CB2 receptor; rCB2, rat CB2 receptor; hADRB2, human β2-adrenergic receptor; hACM3, human muscarinic acetylcholine receptor M3; bRho, bovine rhodopsin; hV1aR, human vasopressin 1a receptor; hOPRD, human δ-type opioid receptor; tADRB1, turkey β1-adrenergic receptor; hD2DR, human dopamine D2 receptor. The CB1 EC2 region and flanking residues were defined based on the crystal structures of the β2-adrenergic receptor (Cherezov et al., 2007). Green and red residues are indicated as described at the top (A). The phenylalanine of the Cys-X-X-X-Ar motif is highlighted in blue. C, illustration of molecular model of the human CB1 receptor from an expanded extracellular view. The molecular model of the human CB1 receptor has been derived from the X-ray crystal structure of the β2-adrenergic receptor. The TM helices are colored as: TM1 (blue), TM2–TM3 (cyan), TM4–TM5(green), and TM6–TM7(yellow/orange). The residues from EC1 are cyan (His178 and Phe189); EC2 are (Trp255, Asn256, Phe268, Pro269, and Ile271). D, a putative binding pocket for CP55940 (gray) within the model of the human CB1 receptor. The TM helices are colored as in C. Several key contact residues for CP55940 are illustrated (fuchsia), including the previously proposed contact points Lys192 and Ser383.

tral to the receptor interior (e.g., Phe268, Pro269, and Ile271). In addition to its projection into the core of the receptor, the position of Phe268 seems to be coordinated by residues of EC1 (e.g., His178 and Phe189) (Fig. 1C).

Docking of the nonclassic agonist CP55940 into the receptor resulted in a number of different binding modes with such similar energetics that it was difficult to choose a preferred binding mode. A lack of a clear, energetically defined mode of ligand binding has been described previously for CP55940 and CB1 in the literature (Salo et al., 2004). One of the binding arrangements, with the C3-alkyl chain of CP55940 projecting extracellularly, is displayed in Fig. 1D. In this binding mode, a number of residues are contributing to the association of CP55940, including Lys192, Val196, Leu359, Met363, Ser383, and Cys386. During the molecular dynamics simulations with the bound CP55940, the EC2 folds over the transmembrane core of the receptor, particularly the α-helical region, with Phe268 plunging more deeply into the core of the receptor and with a "hydrophobic cap" forming on top of the ligand.

Alanine Scanning Mutagenesis of EC2 Identifies Residues Critical for Ligand Binding and Receptor Function. To evaluate the importance of the residues of EC2 in ligand binding and intramolecular interactions as suggested by molecular modeling, each residue (except for Cys257 and Cys264) was individually mutated to alanine, expressed in HEK293T cells, and evaluated for ligand binding with CP55940. The Cys257 and Cys264 were not characterized in this study because previous results indicate that the disulfide bond between these cysteines is required for ligand binding (Shire et al., 1996; Fay et al., 2005). The K_i values for the mutant receptors determined from CP55940 homologous competition assays are presented in Table 1. Alanine substitution of the residues located in the central

region of the loop (i.e., position 258–267) and at position 272 yielded receptors exhibiting an affinity for CP55940 comparable with, or somewhat higher than, that of the wild-type CB1 receptor (K_i = 2.6 nM). Three-fold higher affinity of S262A and S265A receptors apparently does not reflect constitutive activity because the EC_{50} value for GTPγS binding and the affinity for the inverse agonist SR141716A did not show a significant shift but rather remained comparable with that of the wild-type receptor. It is possible that for these mutant receptors, there is some structural consequence in EC2 that affects CP55940 binding that is not transmitted throughout the receptor to yield a corresponding change to high affinity G-protein coupling. The B_{max} values (Table 1) for the mutant receptors that bound CP55940 suggested that expression was comparable with that of the wild-type receptor (B_{max} = 3825 ± 80 fmol/mg).

In contrast, CB1 was highly sensitive to mutation of both membrane proximal regions of EC2 (with the exception of D272A) and the W255A, N256A, F268A, P269A, H270A, and I271A receptors exhibited substantially impaired CP55940 binding. Because these mutant receptors did not show any specific binding using 4 nM radioligand tracer, we increased the tracer concentration 5-fold and still only observed displacement of 18 to 44% by the W255A, N256A, F268A, P269A, H270A, and I271A receptors with 32 μM competing unlabeled CP55940 (see Table 1).

To assess the effect of EC2 mutations on the functional properties of the receptors, the ability of the agonist, CP55940 to stimulate the binding of [^{35}S]GTPγS was measured as a marker of receptor activation. Consistent with CP55940 binding properties, alanine substitution of the residues in the central region of the loop and at position 272 did not disrupt G protein coupling of these mutant receptors; EC_{50} values ranging from 2.03 to 9.47 nM (EC_{50} value of

TABLE 1

Affinity and activity data for the wild-type and EC2 mutant receptors using CP55940 and GTPγS binding studies

Data are the median and corresponding 95% confidence limits or the mean ± S.E.M. of three independent experiments performed in duplicate. K_i values were determined from competition binding assays using [^{3}H]CP55940. B_{max} values were determined from saturation binding assays using [^{3}H]CP55940. EC_{50} and E_{max} values were determined from the CP55940 dose-response model.

Receptor	CP55940		GTPγS	
	K_i	B_{max}	EC_{50}	E_{max}
	nM	*fmol/mg*	*nM*	*%WT*
Wild-type	2.6 (1.5–4.6)	3825 ± 80	2.80 (0.87–8.74)	100.0 ± 5.2
W255A	N.D.[a]	N.D.	24.9 (14.2–43.6)*	11.5 ± 2.8*
N256A	N.D.[b]	N.D.	N.D.	N.D.
E258A	3.4 (2.9–3.9)	4898 ± 169	2.53 (0.98–6.53)	86.7 ± 3.7
K259A	2.6 (2.0–3.3)	4964 ± 198	3.91 (1.74–8.75)	84.9 ± 3.1
L260A	3.6 (2.8–4.8)	4996 ± 258	5.84 (3.56–9.60)	85.6 ± 3.9
Q261A	2.6 (2.0–3.4)	4566 ± 163	3.19 (1.64–6.21)	90.6 ± 4.6
S262A	0.8 (0.7–1.0)*	2605 ± 102	9.47 (5.84–15.3)	117.4 ± 5.3
V263A	2.2 (1.7–2.9)	3046 ± 197	2.81 (1.75–4.52)	83.5 ± 1.7
S265A	0.7 (0.4–1.2)*	3106 ± 142	6.46 (4.08–10.22)	89.9 ± 4.6
D266A	1.4 (1.0–2.0)	4665 ± 150	2.03 (0.64–6.46)	88.6 ± 4.8
I267A	1.8 (1.2–2.6)	2408 ± 57	3.58 (1.97–6.51)	88.5 ± 3.9
F268A	N.D.[a]	N.D.	226.6 (97.7–525.6)*	10.2 ± 3.2*
P269A	N.D.[c]	N.D.	41.1 (30.9–53.8)*	22.9 ± 6.4*
H270A	N.D.[d]	N.D.	176.6 (69.9–452.3)*	19.0 ± 2.8*
I271A	N.D.[e]	N.D.	105.0 (65.8–167.4)*	27.4 ± 5.7*
D272A	3.0 (2.7–3.4)	5103 ± 198	3.85 (1.96–7.55)	102.8 ± 5.0

N.D., no detectable binding.

* Statistically significant differences from wild-type ($p < 0.05$) using analysis of variance followed by Dunn's post hoc test.
[a] 31% displacement was observed at 32 μM CP55940 in presence of 20 nM [^{3}H]CP55940 as tracer.
[b] 18% displacement was observed at 32 μM CP55940 in presence of 20 nM [^{3}H]CP55940 as tracer.
[c] 44% displacement was observed at 32 μM CP55940 in presence of 20 nM [^{3}H]CP55940 as tracer.
[d] 39% displacement was observed at 32 μM CP55940 in presence of 20 nM [^{3}H]CP55940 as tracer.
[e] 26% displacement was observed at 32 μM CP55940 in presence of 20 nM [^{3}H]CP55940 as tracer.

wild-type = 2.80 nM) were observed (Table 1). However, a 10-fold increase or more in EC_{50} values were observed with the W255A, N256A, F268A, P269A, H270A, and I271A receptors with considerably reduced E_{max} values (E_{max} values of 0 to 11.5% by the W255A, N256A, and F268A receptors; 19 to 27.4% by P269A, H270A, and I271A receptors) (Table 1). These changes in CP55940 concentration-dependent G protein stimulation paralleled the agonist binding affinity data, suggesting two distinct regions of EC2 are critical for CP55940 sensitivity.

Because no detectable binding for the agonist CP55940 was observed for the W255A, N256A, F268A, P269A, H270A, and I271A receptors, the inverse agonist SR141716A was used to further assess the pharmacological significance of those two distinct regions (Fig. 2). The affinity of the inverse agonist to three mutant receptors, P269A, H270A, and I271A, involving substitution in the C-terminal region of the loop remained wild-type with K_i values of 5.3, 6.2, and 2.4 nM, respectively. In contrast, receptors resulting from substitution with alanine at position 255, 256, and 268 did not display detectable binding to this inverse agonist (data comparable with that for the W255A receptor shown in Fig. 2).

Lack of Ligand Binding and Localization Are Correlated for W255A, N256A, F268A Receptors. Because three mutant receptors, W255A, N256A, and F268A, did not bind SR141716A and CP55940 with high affinity, we wanted to determine whether lack of binding per se was at issue (e.g., due to loss of key functional groups for ligand interaction) or cellular localization was aberrant, leading to a loss in ligand binding. For this purpose, we examined the cellular localization of these receptors as C-terminal GFP fusions in HEK293T cells. As shown in Fig. 3, the wild-type receptor was found in endosomes with some expression at the cell surface, in agreement with previous reports for CB1 (Leterrier et al., 2004; Rozenfeld and Devi, 2008). It is noteworthy that the receptors with mutations in the C terminus region of EC2, P269A, H270A, and I271A, which bound SR141716A but not CP55940, showed a localization pattern similar to that of the wild-type, displayed a somewhat higher amount of plasma membrane localization, confirming that those receptors were indeed folded appropriately and trafficked comparable with the wild-type receptor. In addition, the Q261A

receptor (shown as a control), which bound CP55940 (Table 1) as it did wild-type, also had a comparable cellular localization pattern. In marked contrast, the W255A, N256A, and F268A receptors displayed a perinuclear distribution in the cell (Fig. 3) consistent with ER localization.

The Hydrophobic Nature of Phe268 Is Important for Ligand Binding and Receptor Activation. Because Phe268 is a key part of the Cys-X-X-X-Ar motif of EC2 and molecular modeling suggests that this residue is poised to play a critical role in ligand and/or intramolecular interactions (Fig. 1, C and D), we further examined the properties of this residue that are important for ligand binding, receptor activation, and cellular localization. Thus, this phenylalanine was individually substituted with the aromatic amino acids, tyrosine and tryptophan, and a hydrophilic but uncharged amino acid, asparagine, in addition to the alanine substitution described earlier. As shown in Fig. 4, the F268Y receptor retains high-affinity binding for both CP55940 and SR141716A that was indistinguishable from that of the wild-type receptor. It is noteworthy that the F268W mutant receptor also retained high affinity for the inverse agonist SR141716A (K_i = 7.3 nM); however, impaired CP55940 binding was observed with this receptor (no detectable binding was obtained using a homologous competition binding assay and a K_i value of 8.1 μM was obtained from heterologous binding using [³H]SR141716A as tracer), similar to the properties observed for the P269A, H270A, and I271A receptors involving substitution of residues neighboring Phe268. Because the hydrophobicity of tryptophan is effectively much less than tyrosine when the indole is not participating in hydrogen bonding (Rusch and Kendall, 1992), these results suggest that high-affinity CP55940 binding requires a more
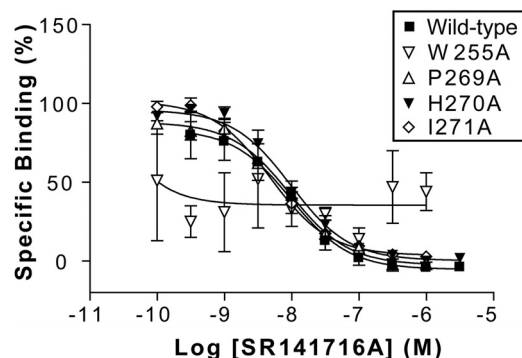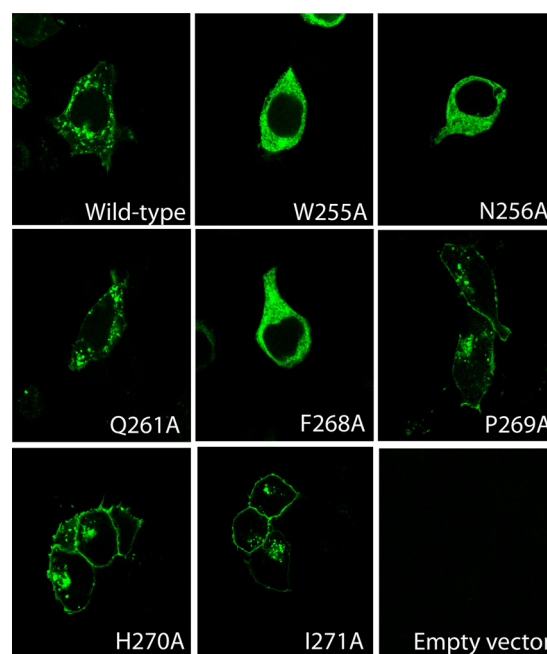

Fig. 3. Cellular distribution of the wild-type and mutant CB1 receptors in HEK293T cells. C-terminally GFP-tagged wild-type and mutant receptors were transiently expressed in HEK293T cells. Forty-eight hours after transfection, cells were fixed and mounted for confocal microscopy as described under *Materials and Methods*. Subcellular distribution of the receptors was assessed by detecting GFP fluorescence. The data are representative images of at least five independent experiments. Empty vector = pcDNA3.1 vector alone (i.e., not carrying the gene for CB1) used to transfect cells as a control. Scale bar, 15 μm.

Fig. 2. Comparison of inverse agonist [³H]SR141716A binding for wild-type and the CB1 mutant receptors that displayed diminished binding to CP55940. Homologous competition binding assays using the CB1 receptor inverse agonist SR141716A were performed on membrane preparations from HEK293T cells expressing the wild-type (■), W255A (▽), P269A (△), H270A (▼), and I271A (◇) receptors. Each data point represents the mean ± S.E.M. of at least three independent experiments performed in duplicate.

hydrophobic residue at this position. When the hydrophobicity and size of this residue was further reduced by substitution with alanine or asparagine, no specific binding of either CP55940 or SR141716A was detected even at 32 μM (Table 2).

To evaluate the involvement of the residue at position 268 on receptor-mediated G protein activation, agonist-induced GTPγS binding was assessed. In agreement with the ligand binding data, the F268Y receptor displayed EC$_{50}$ and E_{max} values comparable with the wild-type receptor (Table 2). The F268W, F268A, and F268N receptors, which displayed very weak or no specific binding of CP55940 showed detectable but markedly increased EC$_{50}$ values ($>$170-fold, $>$80-fold, and $>$160-fold, respectively) and reduced E_{max} values (21.8, 10.2, and 9.8%, respectively) compared with the wild-type receptor.

Cellular Localization of the Receptor Is Influenced by the Nature of the Amino Acid at Position 268. To examine the influence of the amino acid side chain at position 268 on receptor localization, selected Phe268 mutant receptors were expressed in HEK293T cells as C-terminally tagged GFP fusions. As shown in Fig. 5A, the F268Y receptor showed a cellular expression level and intracellular distribution similar to that of the wild-type receptor, whereas the F268W receptor was trafficked and even displayed a somewhat higher amount of plasma membrane localization. In contrast, retention in the perinuclear region was observed for the F268A and F268N receptors, and they were found colocalized with PDI, an ER marker (Fig. 5B) indicating that a somewhat hydrophobic residue at position 268 is required for cellular localization as well as agonist binding.

The C-Terminal Region of EC2 Is Critical for Agonist but Not Inverse Agonist Binding. Because receptors carrying mutations in residues from position 268 through 271 showed impaired binding to CP55940, further ligand binding analyses were performed to assess the pharmacological differences of these receptors relative to the wild-type CB1. For these experiments, the F268W receptor provided an ideal reagent, because it was not trapped in the ER like the F268A receptor and therefore provided a window on possible ligand interactions of the residue at this position. Table 3 summarizes the K_i values for the F268W, P269A, H270A, and I271A receptors and selected CB1 agonists and inverse agonists. [^{3}H]SR141716A was used as a tracer for all ligands evaluated by competition binding assay because high affinity is retained for these mutants and its binding site is thought to overlap with the CB1 agonist CP55940.

The affinity of the F268W, P269A, H270A, and I271A receptors for two structurally similar inverse agonists, SR141716A and AM251, and the structurally distinct inverse agonist, LY320135, was similar to that of wild-type receptor
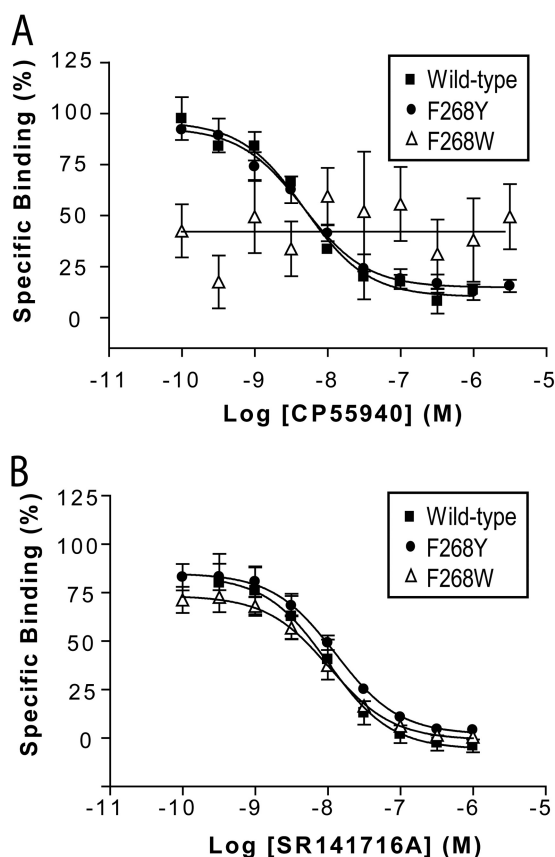

Fig. 4. Comparison of ligand binding for wild-type and the CB1 receptors with mutations at residue 268. Homologous competition binding assays using CB1 receptor agonist CP55940 (A) and inverse agonist SR141716A (B) were performed on membrane preparations from HEK293T cells expressing the wild-type (■), F268Y (●), and F268W (△) receptors. Each data point represents the mean ± S.E.M. of at least three independent experiments performed in duplicate.

TABLE 2

Affinity and activity data for the wild-type and CB1 receptors with mutations at residue 268

Data are the median and corresponding 95% confidence limits or the mean ± S.E.M. of three independent experiments performed in duplicate. B_{max} value for wild-type was 3825 ± 80 fmol/mg as reported in Table 1; B_{max} value for F268Y was 3405 ± 228 fmol/mg. EC$_{50}$ and B_{max} values were determined from CP55940 dose-response model.

Receptor	CP55940			SR141716A K_i
	K_i	GTPγS		
		EC$_{50}$	E_{max}	
	nM	*nM*	*%WT*	*nM*
Wild-type	2.6 (1.5–4.6)	2.80 (0.87–8.74)	100.0 ± 5.2	5.2 (3.4–8.1)
F268Y	2.3 (1.8–3.0)	7.56 (2.48–23.1)	83.1 ± 6.1	9.0 (7.9–10.3)
F268W	N.D.[a]	481.5 (323.7–716.1)*	21.8 ± 2.2*	7.3 (6.4–8.3)
F268A	N.D.[b]	226.6 (97.65–525.6)*	10.2 ± 3.2*	N.D.[c]
F268N	N.D.[d]	465.2 (260.0–832.5)*	9.8 ± 2.7*	N.D.[c]

N.D., no detectable binding up to 100 μM of displacing ligand at 20 nM tracer.
* Statistically significant differences from wild-type ($p < 0.05$) using analysis of variance followed by Dunn's post hoc test.
[a] 26% displacement was observed at 32 μM CP55940 in presence of 20 nM [^{3}H]CP55940.
[b] 31% displacement was observed at 32 μM CP55940 in presence of 20 nM [^{3}H]CP55940.
[d] 28% displacement was observed at 32 μM CP55940 in presence of 20 nM [^{3}H]CP55940.
[c] No displacement was observed at 32 μM SR141716A in presence of 40 nM [^{3}H]SR141716A.

$(K_i = 5.2, 2.1,$ and 52.2 nM, respectively) (Fig. 6, A and B; Table 3). In contrast, using [³H]SR141716A as a tracer, we could establish that these receptors display at least a 100-fold increase in K_i value for CP55940 compared with the wild-type receptor (Fig. 6C). These mutant receptors also exhibited a substantial reduction (>6–100-fold) in binding affinity for the classic CB1 agonist HU-210 (Fig. 6D). To test the hypothesis that the observed ligand-binding sensitivity extends broadly to agonists, (R)-N-(2-hydroxy-1-methyl-ethyl)-5Z,8Z,11Z,14Z-eicosatetraenamide (methanandamide), a methylated derivative of the endogenous anandamide and a structurally very different, ligand was also evaluated for binding to the receptors with mutations in the 268 to 271 region. The affinity of the mutants for methanandamide was also significantly reduced compared with the wild-type receptor (Table 3). These data underscore a role for Phe268, Pro269, His270, and Ile271 of EC2 in binding a variety of agonists, perturbation of these residues leading to a loss in agonist binding. The insensitivity of inverse agonist binding to mutations in this region of the receptor suggests that the binding sites for these two classes of compounds are partially distinct.

Discussion

It has been suggested that the role of EC2 is in stabilization of the receptor inactive state (Klco et al., 2005), cell
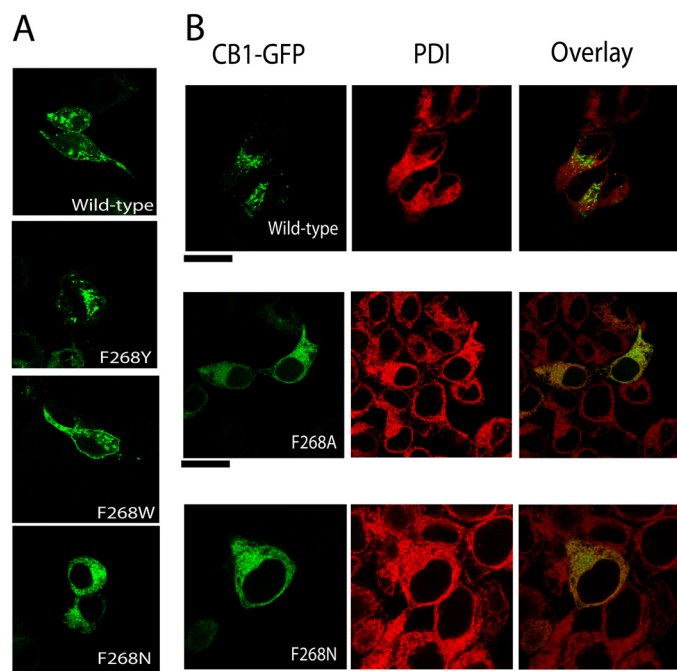
A

B

Fig. 5. Comparison of the subcellular distribution of the wild-type and CB1 receptors with mutations at residue 268. A, subcellular localization of GFP-tagged wild-type and CB1 mutant receptors. HEK293T cells were transiently transfected with GFP-tagged CB1 wild-type or the F268Y, F268W, or F268N receptors. Subcellular distribution of the receptors was assessed by detecting GFP fluorescence. The data are representative images of at least five independent experiments. Scale bar, 15 μm. B, colocalization of GFP-tagged wild-type, F268A, and F268N receptors with the ER marker, PDI, in HEK293T cells. HEK293T cells transiently expressing wild-type, F268A, and F268N receptors were fixed, permeabilized, and stained with antibodies against PDI as described under *Materials and Methods*. Green, GFP fluorescence from receptors (left); red, PDI fluorescence (middle); yellow, colocalization of the receptors and PDI (right). Images were chosen as representatives from at least three independent transfections. Scale bar, 15 μm.

TABLE 3

K_i values for binding of various ligands to CB1 receptors with mutations in the 268 to 271 region of EC2

Data are the median and corresponding 95% confidence limits of three independent experiments performed in duplicate. K_i values for each ligand were determined using 4 nM [³H]SR141716A.

Receptor	CP55940	HU-210	Methanandamide	SR141716A	AM251	LY320135
			K_i			
			nM			
Wild-type	24.8 (14.6–42.3)	3.7 (2.1–6.5)	523 (403–680)	5.2 (3.4–8.1)	2.1 (1.1–4.2)	52.2 (34.3–79.6)
F268W	8132 (5793–11421)*	1672 (757.9–3689)*	20090 (7371–54730)*	7.3 (6.4–8.3)	5.7 (3.9–8.7)	43.4 (34.1–55.2)
P269A	2081 (1256–3446)*	22.6 (10.3–49.5)*	5470 (4319–6927)*	5.3 (3.8–7.3)	2.4 (1.2–4.8)	50.0 (27.3–91.6)
H270A	2576 (1492–4446)*	100 (63–159)*	935 (265–3297)	6.2 (4.4–8.7)	2.0 (1.3–3.1)	70.4 (52.1–95.1)
I271A	3306 (1422–7686)*	310 (117–822)*	41400 (5860–292500)*	2.4 (1.9–2.9)	1.7 (1.1–2.5)	61.2 (46.1–81.1)

N.D., no detectable binding up to 100 μM at 20 nM of [³H]SR141716A.

* Statistically significant differences from wild-type ($p < 0.05$) using analysis of variance followed by Dunn's post hoc test.

surface expression (Hawtin et al., 2006), and/or receptor internalization (Li et al., 2001). The conformational changes noted in molecular models of the loop structure of the V1a vasopressin receptor concurrent with ligand docking (Hawtin et al., 2006), and the constitutive activity that results from many single mutations in EC2 of the complement factor 5a receptor (Klco et al., 2005), support the idea that the loop is integral to receptor activation. It is noteworthy that mutation of two residues within the human GnRH receptor EC2 region led to the conversion, upon binding, of an antagonist to an agonist with biological activity (Ott et al., 2002). Nonetheless, many of these properties are interconnected, and it is often difficult to tease apart 1) issues of cell expression and ligand binding; 2) the direct interaction of an amino acid functional group with ligand versus an intrareceptor interaction that is altered, thereby affecting ligand binding; and 3) the involvement of EC2 residues directly in receptor activation or indirectly through linkage to the critical DRY motif of the C terminus of TM3 for those receptors with a disulfide bridge between TM3 and EC2.

In this study, we took a comprehensive examination of the role of the second extracellular loop of the human CB1 receptor to distinguish its involvement in ligand binding selectivity and receptor localization. The molecular model of the human CB1 receptor developed here gave us a starting point. This model is the first to use the recently solved X-ray structure of the β2-adrenergic receptor (Rasmussen et al., 2007). The major difference with respect to the studies, here is the presence of an α-helix in the central portion of EC2 of the β2-adrenergic receptor, also identified for CB1 that is absent in rhodopsin. In the absence of ligand, the α-helix plus interactions involving Phe268 and EC1 may be needed to assist in stabilizing the ensemble of transmembrane helices during trafficking, whereas CP55940 binding leads to some rearrangements, and EC2 can fold down onto the receptor core and the hydrophobic portion of the ligand. In addition to the

previously proposed contact residues including Lys192, Ser383, and Cys386, our CP55940 docking model suggests that Phe268 is a key part of the capping motif on top of the ligand-binding crevice.

To experimentally probe the role of EC2, we performed alanine scanning mutagenesis of all but the two cysteines at position 257 and 264. The cysteine residues have previously been indirectly shown to be important for cell surface expression (Shire et al., 1996; Fay et al., 2005). The data revealed six residues in two distinct regions of EC2 that exhibited impaired binding affinity and reduced potency for CP55940 relative to the wild-type receptor (Table 1). It is noteworthy that the mutant receptors that showed no detectable binding to CP55940 in ligand binding analyses showed markedly reduced EC_{50} and very low, but detectable, E_{max} values. It is possible that a very small population of folded mutant receptor could respond at a higher concentration of CP55940. All six residues identified here are defined in other studies as part of EC2 (Kapur et al., 2007; Padgett et al., 2008), yet clustered at either the N terminus (Trp255 and Asn256) or C terminus (Phe268, Pro269, His270, and Ile271) of the loop, suggesting that they may play a role as two units, rather than influence ligand binding through an interaction with a single amino acid functional group.

Further analysis of cells expressing the W255A and N256A receptors using confocal microscopy revealed that these receptors are expressed but not trafficked; rather, they colocalize with PDI, a marker of the ER (data not shown). The Trp255 and Asn256 residues are located between the membrane interface and the cysteine at position 264 that contributes to the intraloop disulfide bond. It is possible that mutation of these residues affects disulfide bond formation by perturbing the orientation of the cysteine residue at position 257, in turn affecting folding, ultimately receptor trafficking, and therefore ligand binding. However, molecular modeling of the wild-type EC2 sequence suggested that Trp255 is ori-
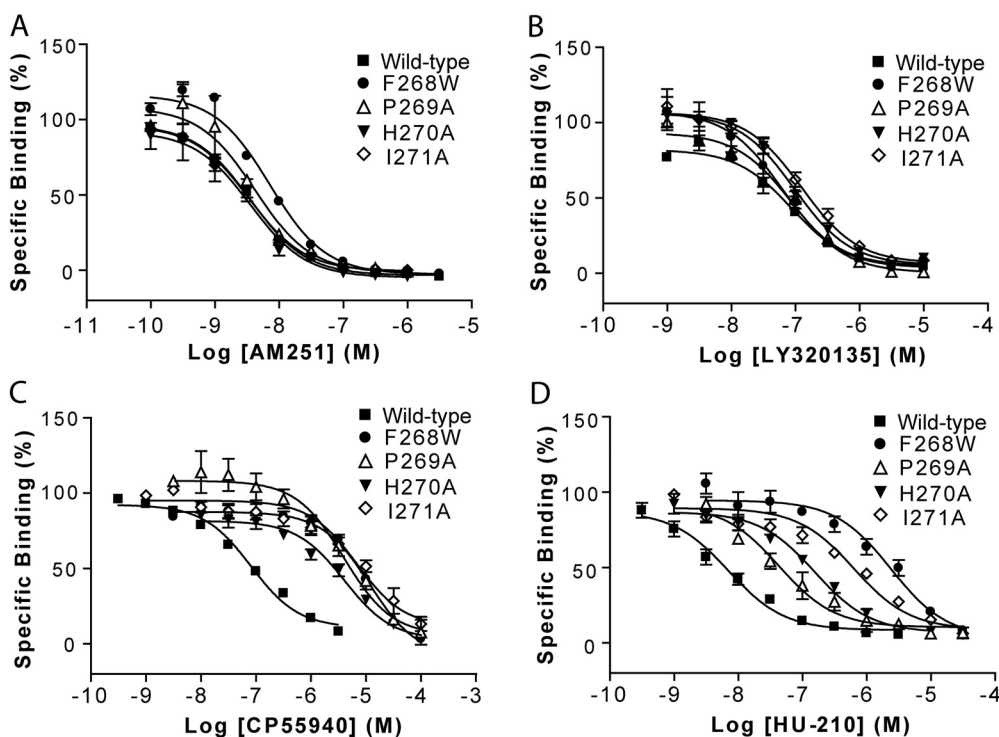
Fig. 6. Competitive displacement of [³H]SR141716A with various ligands by the F268W, P269A, H270A, and I271A mutant receptors. AM251 (A), LY320135 (B), CP55940 (C), and HU-210 (D) were used for displacing 4 nM [³H]SR141716A in membrane preparations from HEK293T cells expressing wild-type (■), F268W (●), P269A (△), H270A (▽), and I271A (◇) receptors. Each data point represents the mean ± S.E.M. of at least three independent experiments performed in duplicate.

ented away from the receptor core in a manner well suited to interact with the surrounding lipid (Fig. 1C). Tryptophan residues are often located at the membrane interface where they can hydrogen bond with the lipid carbonyl groups or interfacial water, effectively anchoring and defining the length of the transmembrane helix (Kelkar and Chattopadhyay, 2006). Mutation of residues at the membrane interface can disrupt these interactions causing a change in the extent of membrane partitioning and consequently structural defects in the protein (Shao et al., 2007), that we show in CB1 preclude trafficking.

In contrast, substitution of the aspartic acid at position 272 for alanine at the C-terminal end of EC2, yielded the D272A receptor with CP55940 binding affinity comparable with that of wild-type receptor. This suggests the impaired binding exhibited by mutation of the neighboring residues to yield the P269A, H270A, and I271A receptors is not due to disruption of interfacial interactions but reflects a direct contribution to the ligand binding pocket consistent with molecular modeling (Fig. 1, C and D).

In addition to the W255A and N256A mutant receptors, the F268A receptor failed to bind both the agonist CP55940 and inverse agonist SR141716A in a practical concentration range and exhibited ER retention. These data support the possibility that EC2 also plays a role as a determinant for receptor folding, thus affecting proper trafficking of the receptor. Molecular modeling of this region highlights the proximity of Phe268 to EC1 and, in particular, residues Phe189 and His178 (Fig. 1C) that may be key contacts. Substitution of Phe268 with the polar residue asparagine also resulted in ER retention of the receptor (and no detectable CP55940 or SR141716A binding), whereas substitution with the hydrophobic aromatic residue tyrosine yielded receptors that exhibited similar ligand binding (Fig. 4) and cellular localization (Fig. 5) comparable with that of the wild-type receptor. The hydrophobicity of the amino acid at this position seems critical for the interactions that lead to proper cellular trafficking.

Remarkably, analysis of the properties of the F268W receptor provided a window for distinguishing the role of the residue at this position in cellular trafficking versus ligand binding. The F268W receptor was localized to the cell surface, bound SR141716A yet not CP55940, results similar to those obtained with receptors with mutations in the neighboring residues, P269A, H270A, and I271A. These data argue that Phe268 functions in both receptor assembly and in binding of agonist, and interactions with neighboring residues are involved. It is noteworthy that modeling of EC2 in the absence of ligand suggested that residues in EC1 are potential points of interaction with Phe268 (Fig. 1C), and during molecular dynamics simulations to dock CP55940, the Phe268 plunges more deeply into the internal crevice of the receptor. Although simulations with CP55940 revealed a few different binding modes of comparable energy, in all of these, the movement of EC2 was comparable. Furthermore, the heterocyclic portion of the ligand bound in a similar fashion, whereas the position of the hydrocarbon tail differed more extensively in agreement with an earlier CB1 model based on rhodopsin (Salo et al., 2004). Previous mutagenesis studies (Song and Bonner, 1996; Chin et al., 1998) have demonstrated that Lys192 of CB1 is important for CP55940 binding and our model (Fig. 1D) as well as others (Shim et al., 2003;

Salo et al., 2004) place this residue within hydrogen bonding distance of CP55940. In contrast, although residues Glu258, Lys259, Gln261, and Asp266 of EC2 may be involved in a hydrogen bond network, as suggested previously (Shim et al., 2003), our finding that substitution of these with alanine does not impair receptor affinity for CP55940 suggests that these residues are not of primary importance in binding of this agonist or trafficking.

Further ligand binding analyses revealed that receptors with mutations in the C terminus region of EC2 bound the inverse agonists SR141716A, AM251, and LY320135 but did not bind any of the three agonists tested. These include 1) the nonclassic cannabinoid CP55940, a bicyclic compound with a hydrocarbon tail that retains the affinity of Δ^9-THC for the wild-type receptor but lacks the pyran ring, making it less lipophilic; 2) HU-210, which is a tricyclic dibenzopyran derivative that incorporates an additional hydroxyl not found in Δ^9-THC; and 3) methanandamide, an analog of the endogenous ligand anandamide, which is less prone to hydrolysis by fatty acid amide hydrolase yet retains the long polyene hydrocarbon chain of anandamide but not the cyclic ring structure of other agonists. This suggests a role for these EC2 residues in accommodating the entry and/or final docking of the long hydrocarbon tail that is shared by the agonists but not the inverse agonists. The pharmacological analyses performed here highlight the significance of the EC2 loop in both intramolecular interactions for proper membrane assembly and trafficking and in ligand-selective interactions. Because the latter interactions distinguish agonist and inverse agonist binding, these data should be valuable for the selective development of therapeutic agents.

References

Abadji V, Lucas-Lenard JM, Chin C, and Kendall DA (1999) Involvement of the carboxyl terminus of the third intracellular loop of the cannabinoid CB1 receptor in constitutive activation of Gs. *J Neurochem* **72:**2032–2038.
Chen C and Okayama H (1987) High-efficiency transformation of mammalian cells by plasmid DNA. *Mol Cell Biol* **7:**2745–2752.
Cheng Y and Prusoff WH (1973) Relationship between the inhibition constant (K1) and the concentration of inhibitor which causes 50 per cent inhibition (I50) of an enzymatic reaction. *Biochem Pharmacol* **22:**3099–3108.
Cherezov V, Rosenbaum DM, Hanson MA, Rasmussen SG, Thian FS, Kobilka TS, Choi HJ, Kuhn P, Weis WI, Kobilka BK, et al. (2007) High-resolution crystal structure of an engineered human beta2-adrenergic G protein-coupled receptor. *Science* **318:**1258–1265.
Chin CN, Lucas-Lenard J, Abadji V, and Kendall DA (1998) Ligand binding and modulation of cyclic AMP levels depend on the chemical nature of residue 192 of the human cannabinoid receptor 1. *J Neurochem* **70:**366–373.
Conner M, Hawtin SR, Simms J, Wootten D, Lawson Z, Conner AC, Parslow RA, and Wheatley M (2007) Systematic analysis of the entire second extracellular loop of the V(1a) vasopressin receptor: key residues, conserved throughout a G-protein-coupled receptor family, identified. *J Biol Chem* **282:**17405–17412.
Fay JF, Dunham TD, and Farrens DL (2005) Cysteine residues in the human cannabinoid receptor: only C257 and C264 are required for a functional receptor, and steric bulk at C386 impairs antagonist SR141716A binding. *Biochemistry* **44:**8757–8769.
Hawtin SR, Simms J, Conner M, Lawson Z, Parslow RA, Trim J, Sheppard A, and Wheatley M (2006) Charged extracellular residues, conserved throughout a G-protein-coupled receptor family, are required for ligand binding, receptor activation, and cell-surface expression. *J Biol Chem* **281:**38478–38488.
Holtmann MH, Hadac EM, and Miller LJ (1995) Critical contributions of amino-terminal extracellular domains in agonist binding and activation of secretin and vasoactive intestinal polypeptide receptors. Studies of chimeric receptors. *J Biol Chem* **270:**14394–14398.
Howlett AC, Barth F, Bonner TI, Cabral G, Casellas P, Devane WA, Felder CC, Herkenham M, Mackie K, Martin BR, et al. (2002) International Union of Pharmacology. XXVII. Classification of cannabinoid receptors. *Pharmacol Rev* **54:**161–202.
Kapur A, Hurst DP, Fleischer D, Whitnell R, Thakur GA, Makriyannis A, Reggio PH, and Abood ME (2007) Mutation studies of Ser7.39 and Ser2.60 in the human CB1

cannabinoid receptor: evidence for a serine-induced bend in CB1 transmembrane helix 7. *Mol Pharmacol* **71:**1512–1524.

Karnik SS, Sakmar TP, Chen HB, and Khorana HG (1988) Cysteine residues 110 and 187 are essential for the formation of correct structure in bovine rhodopsin. *Proc Natl Acad Sci U S A* **85:**8459–8463.

Kelkar DA and Chattopadhyay A (2006) Membrane interfacial localization of aromatic amino acids and membrane protein function. *J Biosci* **31:**297–302.

Klco JM, Wiegand CB, Narzinski K, and Baranski TJ (2005) Essential role for the second extracellular loop in C5a receptor activation. *Nat Struct Mol Biol* **12:**320–326.

Leterrier C, Bonnard D, Carrel D, Rossier J, and Lenkei Z (2004) Constitutive endocytic cycle of the CB1 cannabinoid receptor. *J Biol Chem* **279:**36013–36021.

Li S, Liu X, Min L, and Ascoli M (2001) Mutations of the second extracellular loop of the human lutropin receptor emphasize the importance of receptor activation and de-emphasize the importance of receptor phosphorylation in agonist-induced internalization. *J Biol Chem* **276:**7968–7973.

López de Maturana R, Willshaw A, Kuntzsch A, Rudolph R, and Donnelly D (2003) The isolated N-terminal domain of the glucagon-like peptide-1 (GLP-1) receptor binds exendin peptides with much higher affinity than GLP-1. *J Biol Chem* **278:**10195–10200.

McAllister SD, Rizvi G, Anavi-Goffer S, Hurst DP, Barnett-Norris J, Lynch DL, Reggio PH, and Abood ME (2003) An aromatic microdomain at the cannabinoid CB(1) receptor constitutes an agonist/inverse agonist binding region. *J Med Chem* **46:**5139–5152.

Montero C, Campillo NE, Goya P, and Páez JA (2005) Homology models of the cannabinoid CB1 and CB2 receptors. A docking analysis study. *Eur J Med Chem* **40:**75–83.

Murphy JW and Kendall DA (2003) Integrity of extracellular loop 1 of the human cannabinoid receptor 1 is critical for high-affinity binding of the ligand CP 55,940 but not SR 141716A. *Biochem Pharmacol* **65:**1623–1631.

Ott TR, Troskie BE, Roeske RW, Illing N, Flanagan CA, and Millar RP (2002) Two mutations in extracellular loop 2 of the human GnRH receptor convert an antagonist to an agonist. *Mol Endocrinol* **16:**1079–1088.

Padgett LW, Howlett AC, and Shim JY (2008) Binding mode prediction of conformationally restricted anandamide analogs within the CB1 receptor. *J Mol Signal* **3:**5.

Palczewski K, Kumasaka T, Hori T, Behnke CA, Motoshima H, Fox BA, Le Trong I, Teller DC, Okada T, Stenkamp RE, et al. (2000) Crystal structure of rhodopsin: A G protein-coupled receptor. *Science* **289:**739–745.

Pellegrini M, Bremer AA, Ulfers AL, Boyd ND, and Mierke DF (2001) Molecular characterization of the substance P*neurokinin-1 receptor complex: development of an experimentally based model. *J Biol Chem* **276:**22862–22867.

Phillips JC, Braun R, Wang W, Gumbart J, Tajkhorshid E, Villa E, Chipot C, Skeel RD, Kalé L, and Schulten K (2005) Scalable molecular dynamics with NAMD. *J Comput Chem* **26:**1781–1802.

Porter AC and Felder CC (2001) The endocannabinoid nervous system: unique opportunities for therapeutic intervention. *Pharmacol Ther* **90:**45–60.

Rasmussen SG, Choi HJ, Rosenbaum DM, Kobilka TS, Thian FS, Edwards PC, Burghammer M, Ratnala VR, Sanishvili R, Fischetti RF, et al. (2007) Crystal structure of the human beta2 adrenergic G-protein-coupled receptor. *Nature* **450:**383–387.

Rosenbaum DM, Cherezov V, Hanson MA, Rasmussen SG, Thian FS, Kobilka TS, Choi HJ, Yao XJ, Weis WI, Stevens RC, et al. (2007) GPCR engineering yields high-resolution structural insights into beta2-adrenergic receptor function. *Science* **318:**1266–1273.

Rozenfeld R and Devi LA (2008) Regulation of CB1 cannabinoid receptor trafficking by the adaptor protein AP-3. *FASEB J* **22:**2311–2322.

Rusch SL and Kendall DA (1992) Signal sequences containing multiple aromatic residues. *J Mol Biol* **224:**77–85.

Salo OM, Lahtela-Kakkonen M, Gynther J, Järvinen T, and Poso A (2004) Development of a 3D model for the human cannabinoid CB1 receptor. *J Med Chem* **47:**3048–3057.

Shao C, Shi X, Wehbi H, Zambonelli C, Head JF, Seaton BA, and Roberts MF (2007) Dimer structure of an interfacially impaired phosphatidylinositol-specific phospholipase C. *J Biol Chem* **282:**9228–9235.

Shi L and Javitch JA (2004) The second extracellular loop of the dopamine D2 receptor lines the binding-site crevice. *Proc Natl Acad Sci U S A* **101:**440–445.

Shim JY, Welsh WJ, and Howlett AC (2003) Homology model of the CB1 cannabinoid receptor: sites critical for nonclassical cannabinoid agonist interaction. *Biopolymers* **71:**169–189.

Shire D, Calandra B, Delpech M, Dumont X, Kaghad M, Le Fur G, Caput D, and Ferrara P (1996) Structural features of the central cannabinoid CB1 receptor involved in the binding of the specific CB1 antagonist SR 141716A. *J Biol Chem* **271:**6941–6946.

Song ZH and Bonner TI (1996) A lysine residue of the cannabinoid receptor is critical for receptor recognition by several agonists but not WIN55212-2. *Mol Pharmacol* **49:**891–896.

Strader CD, Fong TM, Tota MR, Underwood D, and Dixon RA (1994) Structure and function of G protein-coupled receptors. *Annu Rev Biochem* **63:**101–132.

Warne T, Serrano-Vega MJ, Baker JG, Moukhametzianov R, Edwards PC, Henderson R, Leslie AG, Tate CG, and Schertler GF (2008) Structure of a beta1-adrenergic G-protein-coupled receptor. *Nature* **454:**486–491.

Address correspondence to: Debra A. Kendall, Department of Molecular and Cell Biology, 91 North Eagleville Road, University of Connecticut, Storrs, CT 06269-3125. E-mail: debra.kendall@uconn.edu